arXiv:1403.2149v1 [cond-mat.str-el] 10 Mar 2014

An Exact Solution of the PPP Model for Correlated Electronic States of Tetracene and Substituted Tetracene

Y. Anusooya Pati and S. Ramasesha*

Solid State and Structural Chemistry Unit, Indian Institute of Science, Bangalore 560 012, India

E-mail: ramasesh@sscu.iisc.ernet.in

*To whom correspondence should be addressed

Abstract

Tetracene is an important conjugated molecule for device applications. We have used the diagrammatic valence bond method to obtain the desired states, in a Hilbert space of about 450 million singlets and 902 million triplets. We have also studied the donor/acceptor (D/A) substituted tetracenes with D and A groups placed symmetrically about the long axis of the molecule. In these cases, by exploiting a new symmetry, which is a combination of C_2 symmetry and electron-hole symmetry, we are able to obtain their low-lying states. In the case of substituted tetracene, we find that optically allowed one-photon excitation gaps reduce with increasing D/A strength, while the lowest singlet-triplet gap is only weakly affected. In all the systems we have studied, the excited singlet state, S_1 is at more than twice the energy of the lowest triplet state and the second triplet is very close to S_1 state. Thus donor-acceptor substituted tetracene could be a good candidate in photo-voltaic device application as it satisfies energy criteria for singlet fission. We have also obtained the model exact second harmonic generation (SHG) coefficients using correction vector method and we find that the SHG responses increase with the increase in D/A strength.

Introduction

There is an increased interest in the study of polycyclic hydrocarbons, particularly, tetracene and pentacene since the last decade due to their large hole mobility and improved field effect transistor (FET) efficiencies.[1] They are used in Organic Light Emitting diode (OLED) applications, in field effect transistors and photovoltaic devices. Metal doped pentacenes and picenes show superconductivity at relatively high T_c values (above 7K).[2] These systems are building blocks of graphene and are semiconducting in nature. Organic counterpart of inorganic semiconductors are more easy to process and to tailor for required applications with easy substitution. Substitution by electron donating and withdrawing groups leads to ambipolar materials which are used in organic photovoltaic cells.[3] Longer acenes are found to be less stable and hence there are

efforts to derivatize the parent tetracene and pentacene compounds to make them more soluble and stable.[4] Yutaka et al have synthesized benzopyrazine-fused tetracene compounds and found that these compounds are more photostable and have long wavelength absorption. The major aim is to tune the HOMO - LUMO gap to assist the easy flow of positively charged holes and negatively charged electrons, either for recombination or for charge separation, depending upon the application i.e. LEDs or photovoltaics. One way to reduce the HOMO-LUMO gap is to increase the conjugation length of the molecule and another is to substitute the systems with electron withdrawing and donating groups.[5]

A recent paradigm in the field of organic photovoltaics is the fission of the photoexcited singlet into two triplets.[6–8] These triplets generated by fission can then undergo dissociation to yield twice the number of charge carriers that is produced by singlet dissociation. There are several conditions under which this can happen with larger probability. They are (i) the energy $E(S_1)$ of the lowest excited singlet state, S_1, is greater than or equal to twice the triplet energy ($E(S_1) \geq 2E(T_1)$, (ii) the second triplet state, T_2, is above the singlet excited state, S_1, i.e. ($E(T_2) > E(S_1)$), as this will avoid leaking of the S_1 state to T_2 via intersystem crossings and (iii) $E(T_1)$ should be at least 1 eV as otherwise the operating voltage of the OPVC will drop, resulting in lower efficiency. Polycrystalline tetracene and pentacene molecules have been explored in this context.[9–12] Effect of magnetic field on SF has been studied by Bardeen et al.[13]

There are several theoretical studies of these systems using both semi-empirical and *ab-initio* methods and also by the density matrix renormalization group (DMRG) method.[14–18] The energetics and structural parameters of acene series and their analogues - phenanthrene series, has been studied by Wiberg using the DFT method.[14] They analyze their results by studying quantities like resonance energy, ionization potential and $\sigma-$ and $\pi-$ bond indices. Heinze et al have studied the excitation energies and oscillator strengths of acenes using their method based on time dependent density functional theory (TDDFT).[16] Excitation energies of longer acenes

are studied by Kadantsev et al within TDDFT method, both in the singlet and triplet manifold.[15] The triplet-triplet transitions were experimentally measured by Pavlopoulos.[19] Kaur et al studied the effect of substituent on the HOMO-LUMO gaps on pentacene.[20] Aldehyde substituted oligoacenes were studied for their enhanced first order hyperpolarizabilities using hyper Rayleigh scattering technique.[21] The effect of donor-acceptor groups on the first order polarizabilities of substituted oligoacenes were studied within AM1/TDHF method.[22]

The DFT method is basically a ground state method and is helpful for obtaining ground state properties such as molecular geometries. Although the TDDFT method, in principle, can provide excited state information, it suffers from the severe drawback of lack of reliable functionals. Indeed both these methods are similar in line with the well established Hartree-Fock (HF) and TDHF methods which include mean exchange and correlation potentials. All the above methods include both coulomb and exchange correlation, but only at the mean-field level. For obtaining electronic excited state properties for conjugated systems, it has been demonstrated that using a model of π- electrons and treating electron-electron interaction with a very high level theory gives accurate excited states and their properties.[23] In this spirit, we have employed the Pariser-Parr-Pople (PPP) model for describing π electrons. The PPP model includes long-range electron-electron interactions and is suited for semiconducting systems.

In this paper, we have studied tetracene and its donor-acceptor substituted compounds by solving the PPP model exactly using a diagrammatic valence bond (DVB) approach.[24,25] Tetracene molecule consists of 18 $\pi-$ electrons delocalized over the 18 Carbon atoms of tetracene. The full configuration space of tetracene spans over 0.9 billion configurations for triplets, without taking into account the three fold spin degeneracy of triplets and extends DVB calculations to nearly a billion valence bond functions. We have computed excitation energies of these compounds and analyzed their oscillator strengths and geometries both in the ground state and excited states. Besides, we have also explored the triplet states of these systems in the context of singlet fission. We have obtained the model exact SHG response of these systems using the

correction vector techniques. In what follows, we give a brief introduction to the DVB method and model Hamiltonian used, followed by results and discussion.

Methodology

The PPP model assumes $\sigma-\pi$ separability and considers a single p_z orbital at each carbon site, for tetracene this translates to a problem of 18 electrons on 18 site. The PPP Hamiltonian in second quantization notation, with $a^{\dagger}_{i\sigma}$ ($a_{i\sigma}$) creating (annihilating) an electron with spin σ in orbital (site) i with n_i being corresponding occupation number operator, is given by

$$\begin{aligned} H &= \sum_{<i,j>\sigma} t_{ij}(a^{\dagger}_{i\sigma}a_{j\sigma}+a^{\dagger}_{j\sigma}a_{i\sigma})+ \\ &+\sum_i \varepsilon_i n_i+\frac{1}{2}\sum_i U_i n_i(n_i-1) \\ &+\sum_{i>j} V_{ij}(n_i-z_i)(n_j-z_j) \end{aligned} \tag{1}$$

The first term in the Hamiltonian corresponds to the kinetic energy. t_{ij}s are the resonance/hopping (transfer) integrals between bonded carbon sites i and j. The second term corresponds to the site energy with ε_i being the orbital energy of the p_z orbital on the i^{th} carbon atom. U_is are the on-site electron-electron repulsion parameter (the Hubbard parameter) at site i and V_{ij}s are intersite electron-electron repulsion parameters between sites i and j. z_i is the local chemical potential at site i which is 1 for carbon $\pi-$ orbitals. The parameters t_{ij}s are taken as -2.4 eV and U_is are 11.26 eV and V_{ij}s are obtained using the Ohno[26] interpolation formula,

$$V_{ij}=\frac{U_i}{\sqrt{(1.0+0.6117r_{ij}^2)}} \tag{2}$$

where r_{ij} is the intersite distance in Å. Site energy ε is taken as zero for unsubstituted C atoms. We have mimicked the effect of substitution by donors or acceptors at a site i by changing the site energies of the carbon atoms at these sites. Donor site has a +ve site energy while an acceptor site has a negative site energy. We have assumed equal strength of donors and acceptors and varied the magnitude of site energy $|\varepsilon|$ from 2.0 to 4 eV. We have introduced the substituents such that they are at sites related by the C_2 axis along the length of the molecule as shown in 1.

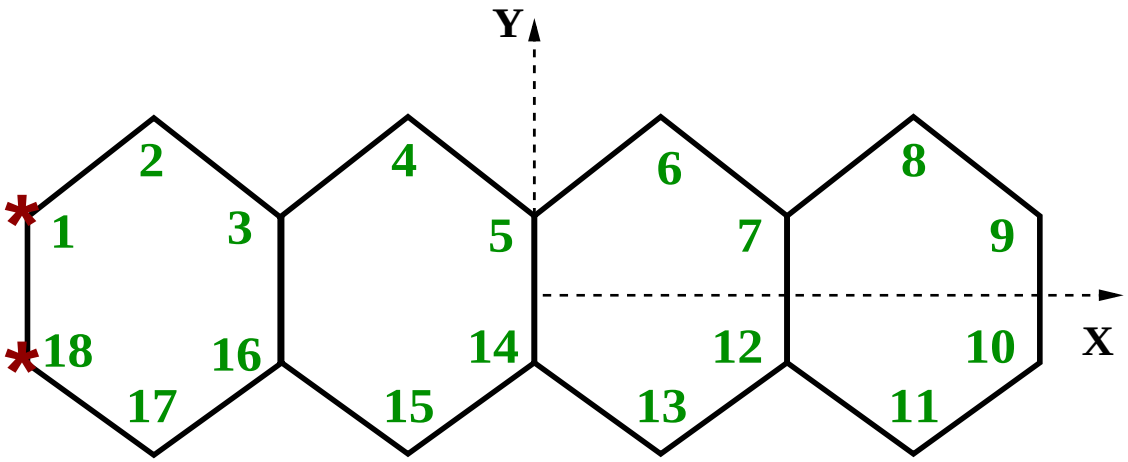

Figure 1: Schematic structure of tetracene. The sites 1 and 18 are substituted by donor and acceptor ($+\varepsilon$ and $-\varepsilon$), respectively.

The unsubstituted tetracene molecule, has spatial symmetry (C_2) and electron-hole symmetry (*e-h*) assuming all carbon sites are identical, leading to an Abelian group of 4 elements. Both these symmetries are broken, when we introduce donor and acceptors in the system. However, if the donor and acceptors are at sites related by 180° rotation about the long axis of the molecule and if the magnitude of donor-acceptor strengths are the same, we will still retain the symmetry corresponding to $C_2 \times$ *e-h*. This can be seen by noting that the C_2 symmetry interchanges sites j and $(N+1)-j$, where $N = 18$ in tetracene. The *e-h* symmetry transforms the creation operator $a_i^\dagger$ at site i to annihilation operator a_i, while at site $(N+1)-i$ it interchanges $a^\dagger_{(N+1)-i} = -a_{(N+1)-i}$ since sites i and $(N+1)-i$ belong to different sublattices. At

half-filling the interaction terms and transfer terms in the substituted tetracene are the same as those in the unsubstituted tetracene and hence their invariance under $C_2 \times e$-h operator is well established. The only additional term is the site energy term $\sum_i \varepsilon_i n_i$ and for substitutions at sites j and $(N+1)-j$, the summation can be written explicitly as $\varepsilon_j n_j + \varepsilon_{(N+1)-j} n_{(N+1)-j}$. Since we impose equal donor and acceptor strengths $\varepsilon_j = -\varepsilon_{(N+1)-j}$ and site energy terms reduce to $\varepsilon_j n_j - \varepsilon_{(N+1)-j} n_{(N+1)-j}$. Operating on this by e-h leads to $-\varepsilon_j n_j + \varepsilon_{(N+1)-j} n_{(N+1)-j}$ and C_2 operation on this term restores the original term in the Hamiltonian. By employing this symmetry for symmetrically substituted donor-acceptor groups in tetracene, we can reduce the Hilbert space dimension, approximately, by half. The largest subspace we have dealt with corresponds to the triplet space of tetracene with symmetric substitution which has a dimension of ≈ 0.45 billion. The valence bond (VB) technique for solving the PPP Hamiltonian is followed along the lines described in earlier work.[24,25]

Results and Discussion

Singlet State Properties

In the case of tetracene, we have obtained a few low-lying singlet and triplet states in the A^+ and B^- subspaces. In the case of substituted tetracene, we have computed a few low-lying states in the Σ and τ subspaces where Σ corresponds to even subspace and τ to the odd subspace, under $C_2 \times e$-h. In substituted tetracenes, it is worth noting that the optical transitions are allowed between states within the same subspaces i.e. $\Sigma \rightarrow \Sigma$ or $\tau \rightarrow \tau$, besides the usual $\Sigma \rightarrow \tau$ transitions. The $\Sigma \rightarrow \Sigma$ transitions are polarized along the short-axis (Y-axis) of the molecule while the $\Sigma \rightarrow \tau$ transitions are polarized along the long axis (X-axis) of the molecule.

Tetracene molecule has D_{2h} symmetry. We have assumed planar geometry and have ignored the Hydrogen atoms. Therefore, the symmetry reduces to D_2, since $C_2(Z)$ is the same as inver-

sion, for a planar molecule. The states of tetracene can therefore be classified as A^+, B_1^+, B_2^+, B_3^+, A^-, B_1^-, B_2^- and B_3^- where the superscripts $+$ and $-$ refer to the electron-hole symmetry, $+$ for even space and $-$ for odd space, representing covalent and ionic spaces. Since we have not used the C_2 symmetry along the Y-axis, to uniquely assign the state lables, we have used the direction of polarization of the transition dipole between the ground state and excited states. The transition to B_1 is Z-polarized and will be disallowed as the molecule is in the XY-plane. Transitions to B_2 states are $Y-$ polarized and to B_3 states are $X-$ polarized.

Table 1: Low-lying singlet-singlet excitations in tetracene as a function of site energy, ε. Energies are in eV and transition dipole moments are in Debye. Σ corresponds to the even space and τ to odd space under $C_2 \times e$-h symmetry. The number with $\star$ is obtained by introducing a small site energy at inequivalent sites of tetracene.[27]

ε		Excited State index						
		1	2	3	4	5	6	7
0.0	gap	3.18 (B_2^-)	—	3.59 (B_1^+)	3.97 $\star$ (B_3)	4.14 (B_1^-)	4.95 (B_3^-)	4.99 (B_3^-)
	μ_x	0.00	—	0.00	0.04	0.00	11.45	1.32
	μ_y	3.74	—	0.00	—	0.00	0.00	0.00
		[2.71][28]	—	—	[3.32][28]	—	[4.52][28]	—
		[2.63][29]	—	—	—	—	[4.51][29]	
2.0	gap	2.72 (Σ)	3.06 (Σ)	3.51 (τ)	4.31 (τ)	4.71 (τ)	4.91 (τ)	5.46 (τ)
	μ_x	0.00	0.00	0.69	1.34	1.86	11.05	1.48
	μ_y	3.27	0.13	0.00	0.00	0.00	0.00	0.00
3.0	gap	2.45 (Σ)	3.06 (Σ)	3.41 (τ)	4.24 (τ)	4.65 (τ)	4.86 (τ)	5.35 (τ)
	μ_x	0.00	0.00	0.89	1.63	1.84	10.64	2.82
	μ_y	3.56	0.58	0.00	0.00	0.00	0.00	0.00
4.0	gap	2.20 (Σ)	3.04 (Σ)	3.30 (τ)	4.15 (τ)	4.59 (τ)	4.79 (τ)	5.22 (τ)
	μ_x	0.00	0.00	0.94	1.59	1.31	10.05	4.24
	μ_y	3.75	0.90	0.00	0.00	0.00	0.00	0.00

In 1 we present the low-energy excitations of tetracene ($\varepsilon = 0$) and substituted tetracene ($\varepsilon \neq 0$). The lowest singlet excitation is at 3.04 eV to A^+ state which is a two-photon state. In

the polyacene series, it is known that two-photon state is above one photon state for tetracene, while for pentacene, the two photon state is below the one photon state.[18] Our results seem to indicate that even for tetracene and for pentacene, the two photon state is below the one photon state. The energy gap of 0.14 eV between the two states is too small to definitely state that the two photon state is below one photon state in the crystal as intermolecular interactions will red shift the one photon state more than the two photon state, the former being more ionic.

Optically allowed excitations are to the B_2^- state at 3.18 eV (weaker) and the B_3^- state at 4.95 eV (stronger). Both these excitations are blue-shifted with respect to the experimental values by ≈ 0.5 eV.[28,29] The excitation around 3.3 eV is very very weak and to observe this peak we need to take into account the inequality of C sites in tetracene.[27] If we take a slightly negative site energy ($\varepsilon = -0.15\ \ eV$) for C_3, C_5, C_7, C_{12}, C_{14} and C_{16} and calculate the energy spectrum, we observe a weak peak at 3.97 eV (with a transition dipole of 0.04 Debye), which is 0.65 eV higher than the experimental value.

On introducing substitution, the strong optically allowed state red shifts progressively from 3.18 eV to 2.72 eV, 2.45 eV and 2.20 eV for $\varepsilon = 2.0$, 3.0 and 4.0 eV, respectively. All these excitations are short axis polarized. The next strongest optical excitation is at a gap of 4.95, 4.91, 4.86 and 4.79 eV for $\varepsilon = 0.0$, 2.0, 3.0 and 4.0 eV, respectively. All these excitations are long axis polarized and show a smaller red shift with increasing strength of substitution. For unsubstituted tetracene, the third optically allowed excitation is nearly degenerate with the second excitation with a small transition dipole along the long axis of tetracene. Upon substitution, this state gets blue-shifted. The excitation energy of this level reduces with the increasing ε value, while the transition dipole moment increases, retaining its direction of polarization.

Charge Density

We have computed the charge density and bond orders for these systems both in the ground state and excited states, which have significant transition dipole moments to the ground state. Because of the *e-h* symmetry, the charge density at every carbon site is 1 for an unsubstituted molecule both in the ground state and excited states. In 2, we have given the charge densities for two different site energies, $\varepsilon = 2.0$ eV and $\varepsilon = 4.0$ eV. For site energy, $\varepsilon = 3.0$ eV, we have given the charge density data in supporting information. At the site of the substitution, the charge density difference is large and it slowly varies alternately along the long - axis of the molecule and reaches the value of 1 away from the sites of substitution. This limiting value is attained over shorter distances from the substituted sites for weaker donor-acceptor strengths. For example, the effect of substitution is seen till the second ring in the case of $\varepsilon = 2.0$, whereas, it is spread upto the third ring for $\varepsilon = 4.0$. The magnitude of difference in charge density varies almost linearly with the strength of the site energy. Another interesting observation is that the sum of the charge densities at sites related by C_2 symmetry about the long-axis is 2.0, which is a consequence of the $C_2 \times$ *e-h* symmetry.

In 3, we have given the difference in charge density between the ground state and excited states which are dipole allowed. As expected, the difference is more at the substituted sites and the magnitude of difference is same at the sites related by C_2 symmetry, which is again a consequence of the $C_2 \times$ *e-h* symmetry. In the excited states, the non-zero difference extends to the farthest sites from the substitution sites. This is in contrast to the ground state charge distribution, which is more localized closer to the site of substitution. The magnitude of the difference is larger for the state which has non-zero transition dipole moment along the Y- axis.

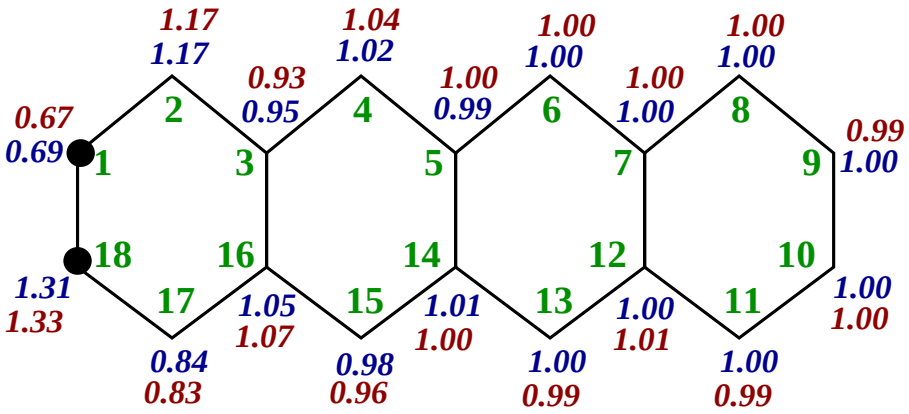

Figure 2: Charge densities for ground state (in blue) and dipole allowed vertically excited state (τ_4, in red) as a function of site energy, ε. (a) for $\varepsilon = 2.0$ eV and (b) for $\varepsilon = 4.0$ eV. Numbers inside the ring in green represent the site/orbital indices.

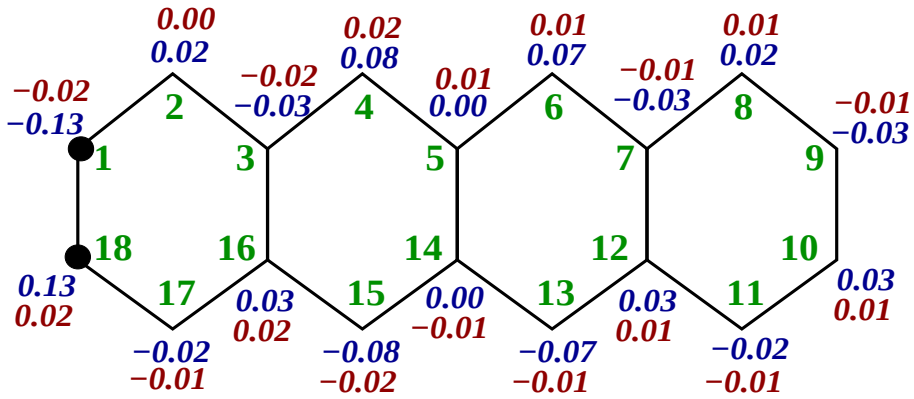

(a)

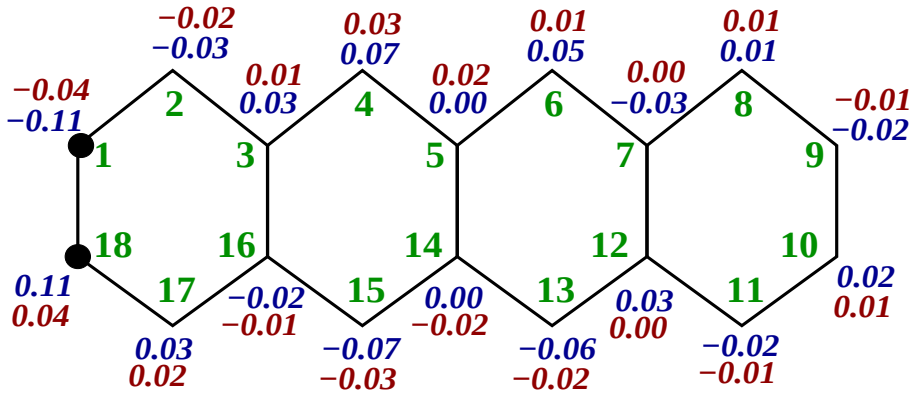

(b)

Figure 3: Difference in charge densities from ground state to vertically excited states in even space (Σ_2, in blue) and odd space (τ_4, in red), as a function of site energy, ε. (a) for $\varepsilon = 2.0$ eV and (b) for $\varepsilon = 4.0$ eV. Numbers inside the ring in green represent the site/orbital indices.

Bond Orders in Singlet states

Bond order p_{ij} of a bond between sites i and j in the state $|\psi>$ is defined as

$$p_{ij} = -\frac{1}{2} < \psi | \sum_{\sigma} a^{\dagger}_{i\sigma} a_{j\sigma} + h.c. | \psi > \tag{3}$$

A larger bond order implies that at equilibrium, the bond would contract while smaller bond order implies the tendency for the bond to elongate. At equilibrium, all bond orders will be proportional to their respective bond lengths, with the same proportionality constant. Thus, a study of the bond order in different states gives an idea of the equilibrium geometry. In 4, we present the bond orders for the ground state (numbers in blue) and excited states (τ_4, numbers in red) for tetracene and substituted tetracenes. In the ground state, outer bonds show strong bond alternation while the inner bonds ($p_{4,5}$ and $p_{5,6}$) tend to be uniform. The rung bonds are weaker and of similar magnitude except in outer most rings (bonds $p_{1,18}$ and $p_{9,10}$). Our bond order patterns compare well with the bond order patterns obtained by Wiberg who computed the Fulton $\pi-$ bond indices for tetracene.[14] The effect of substitution on bond order is more pronounced near the site of substitution, similar to the behavior of charge density.

Upon excitation, the stronger bonds become weaker and vice versa, along the chain and the rung bonds become even more weaker. Moreover, the rung bonds show larger variation compared to the bonds along the chain. In the case of substituted tetracenes, bond order variation is also more localized when the site energy is small and is delocalized when it is large. In all the cases, the excited state geometry is more enlarged than the ground state, since the magnitude of elongation of double bond is larger than the contraction of the single bond. The effect of substitution on bond order is more pronounced near the site of substitution, similar to that observed for charge density behavior.

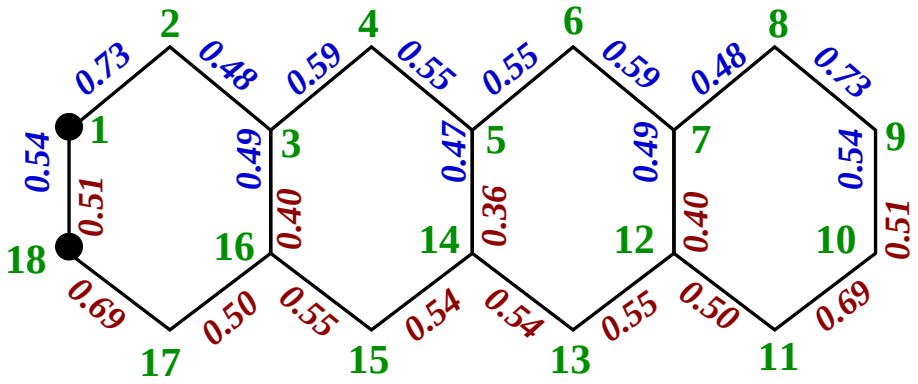

(a)

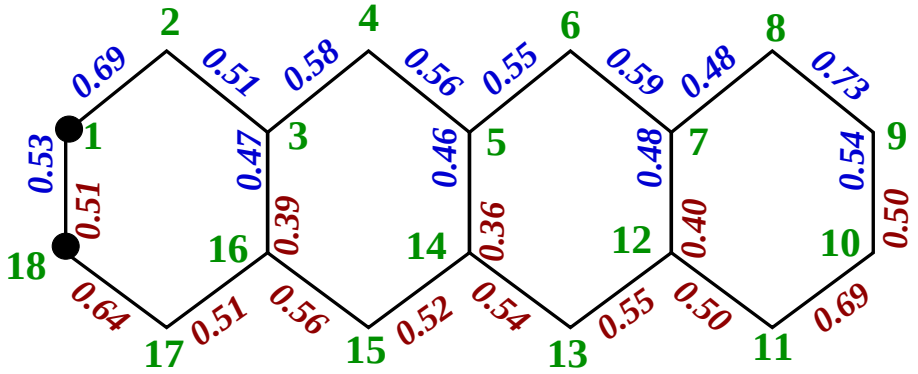

(b)

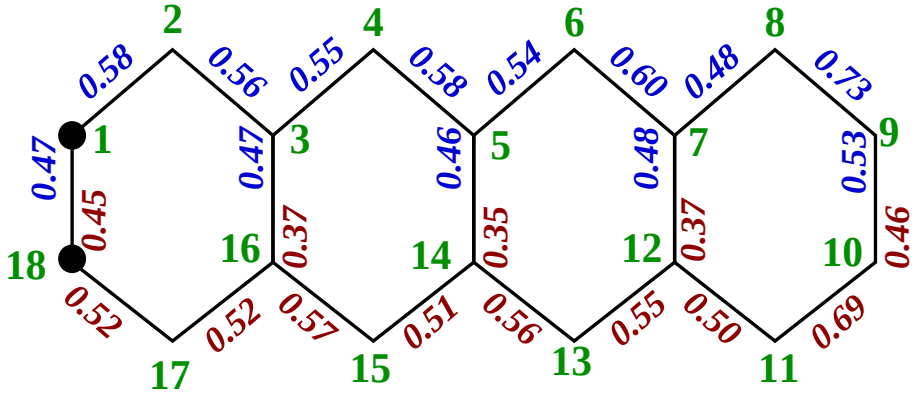

(c)

Figure 4: Bond Order for ground state (Σ_1, in blue) and optically allowed state (τ_4, in red), as a function of site energy, ε. (a) for $\varepsilon = 0.0$ eV, (b) for $\varepsilon = 2.0$ eV and (c) for $\varepsilon = 4.0$ eV. Numbers inside the ring in green represent the site/orbital indices.

Properties of Triplet States

We have computed several excited triplet states in different symmetry subspaces of tetracene and substituted tetracene. Triplet state energies and triplet-triplet transition dipoles are presented in 2. In unsubstituted tetracene, the lowest T-T transition that is optically allowed from T_1 is at 3.07 eV and the transition is long-axis polarized. All the triplet states below this state have no transition dipole for optical excitation. Experimentally two nearly degenerate peaks are observed at 2.61 and 2.70 eV.[19] We observe two more weaker peaks at 3.82 (Y-axis polarized) and 4.50 (X-axis polarized). These peaks are comparable to the experimental peaks at 3.97 eV and 4.36 eV with different polarization axes found experimentally.[19]

On introducing substitution, the lowest T-T transition from T_1 is at ≈ 1.05 eV, independent of the strength of substitution, but the transition dipole increases with increase in substitution strength. This state is not dipole connected to T_1 in unsubstituted tetracene. We observe many weaker peaks (T_2 to T_7) below 3.07 eV of unsubstituted tetracene, all of which are dipole connected to T_1 state. The excitations to T_2, T_3 and T_5 are short-axis polarized for $\varepsilon = 2.0$ and T_2, T_3 and T_6 are short-axis polarized for $\varepsilon = 3.0$ and $\varepsilon = 4.0$ eV. The remaining transitions are long-axis polarized. The transition to T_2, T_3 and T_7 show increase in transition dipole with increasing ε. There seems to be level crossings with ε, for states T_4, T_5 and T_6. For example, T_5 and T_6 seem to cross for $\varepsilon > 2.0$ eV. The strongly allowed T-T transition, T_8, in unsubstituted tetracene becomes progressively weakly allowed, as the substitution strength is increased.

We have compared the singlet-triplet gaps, $E_{S0} - E_{T1}$, $E_{S0} - E_{T2}$ and singlet-singlet gap, $E_{S0} - E_{S1}$ in 3, as a function of site energy, ε. The singlet-triplet gap for the unsubstituted tetracene is 1.22 eV which compares well with the experimental value of 1.25 eV.[30] The triplet or spin gap slightly decreases from 1.22 eV for unsubstituted tetracene to 1.17 eV for $\varepsilon = 2.0$

Table 2: Energy gaps from the lowest triplet state and the corresponding transition dipole moments (Debye) in Tetracene and substituted tetracene as a function of ε. The Even and odd spaces under the $C_2 \times e$-h symmetry are labelled Σ and τ, respectively. All energies are in eV.

ε		Energies of excited states						
		2	3	4	5	6	7	8
0.0	gap	1.05 (B_2)	1.92 (B_2)	1.95 (B_1)	2.46 (B_1)	2.69 (B_1)	2.89 (B_1)	3.07 (B_3)
	μ_x	0.00	0.00	0.00	0.00	0.00	0.00	7.02
	μ_y	0.00	0.00	0.00	0.00	0.00	0.00	0.00
2.0	gap	1.06 (Σ)	1.94 (Σ)	2.03 (τ)	2.39 (Σ)	2.52 (τ)	2.61 (τ)	3.08 (τ)
	μ_x	0.00	0.00	0.33	0.00	3.35	0.94	5.11
	μ_y	0.71	0.47	0.00	0.27	0.00	0.00	0.00
3.0	gap	1.05 (Σ)	1.92 (Σ)	2.09 (τ)	2.36 (τ)	2.40 (Σ)	2.72 (τ)	3.12 (τ)
	μ_x	0.00	0.00	0.08	3.82	0.00	2.02	3.32
	μ_y	1.07	0.68	0.00	0.00	0.29	0.00	0.00
4.0	gap	1.04 (Σ)	1.89 (Σ)	2.11 (τ)	2.24 (τ)	2.45 (Σ)	2.80 (τ)	3.12 (τ)
	μ_x	0.00	0.00	1.52	3.63	0.00	2.64	1.21
	μ_y	1.32	1.17	0.00	0.00	0.21	0.00	0.00

eV, 1.10 and 1.02 eV for $\varepsilon = 3.0$ and 4.0 eV, respectively. In all these cases, the triplet gap is less than half of the lowest singlet gap.

Table 3: Energy levels of T_1, T_2 and S_1, for the tetracene molecule as a function of site energy, ε. All energies are in eV.

ε	T_1	T_2	S_1
0.0	1.22	2.27	3.18
2.0	1.17	2.23	2.72
3.0	1.10	2.15	2.45
4.0	1.02	2.06	2.20

We note from 3 that the energy of the S_1 state is higher than twice the energy of the T_1 state, in all cases. Thus the first condition for singlet fission (SF) is satisfied by both unsubstituted and substituted tetracenes. In the case of unsubstituted tetracenes, the two-photon state is below the one-photon state and two-photon energy is 3.04 eV and this is also more than twice the triplet gap of 1.22 eV. As the donor-acceptor strength is increased, S_1 energy reduces and for $\varepsilon = 4.0$ eV, the S_1 energy is 2.20 eV against a T_1 energy of 1.02 eV. The smaller difference in energy between S_1 and twice T_1 energy implies that less energy is lost to heat in the SF process. Thus strong donor-acceptor substituted tetracenes have an edge over weakly substituted tetracenes. The T_2 state energy of weakly substituted tetracenes is well below the S_1 state. But, for strongly substituted tetracenes, $E(T_2)$ is only 0.14 eV below the S_1 state. These calculations are in the gas phase and intermolecular interactions are expected to reduce the S_1 energy more than T_2 energy and could therefore lead to $E(T_2) > E(S_1)$. The T_1 energies are slightly more than 1 eV implying that the open cell voltage of OPVC will be in the desired range.

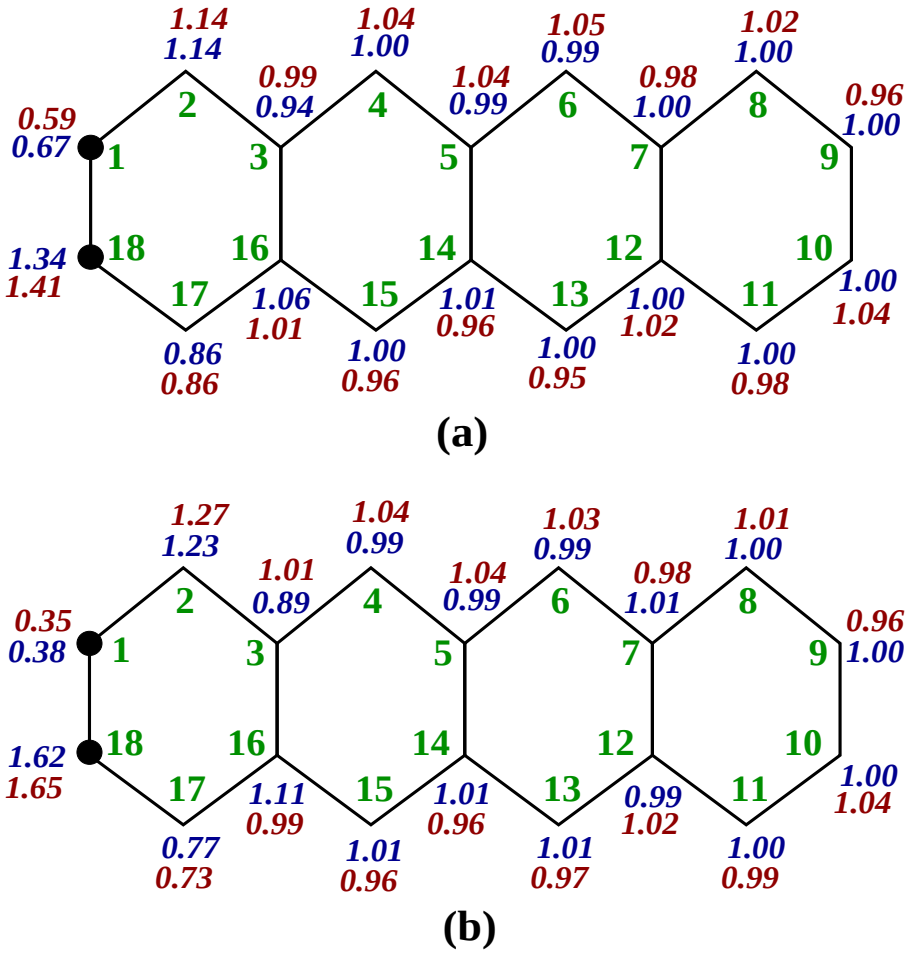

Figure 5: Charge density for ground state (numbers in blue) and optically allowed state (numbers in red, T_2 state), as a function of site energy, ε. (a) for ε = 2.0 eV and (b) for ε = 4.0 eV. Numbers inside the ring in green represent the site/orbital indices.

Charge and Spin Density

The charge densities in triplet states of unsubstituted tetracene are uniform. In the substituted tetracenes, we have shown the charge densities for T_1 and the triplet state to which transition is most intense (T_6 for $\varepsilon = 2.0$ eV and T_5 for $\varepsilon = 3.0eV, 4.0$ eV), in 5 (The charge density data for $\varepsilon = 3.0$ eV is given in supporting information). The charge densities in the T_1 state for all cases show large variation from the mean near the site of substitution. However, unlike in the case of singlets, the charge density fluctuation is more extended, although the change is largest near the site of substitution. In the triplet state with largest transition dipole to the T_1 state, the difference in charge density compared to T_1 is much smaller than in the case of singlets.

We have also computed the spin densities in the T_1 state and the most strongly dipole allowed excited state in both substituted and unsubstituted tetracenes (see 6). Eventhough in substituted tetracenes, the C_2 symmetry about the long axis is broken, the spin densities retain this symmetry. This is because the donor and acceptors have the same substitution strength and spin densities of holes and electrons are the same. The spin densities are all positive except, mainly at sites 5 and 14, eventhough the magnitudes are rather small. The positive spin densities are larger at the interior of tetracene (carbon sites 4, 6, 13 and 15). The spin density magnitudes are rather weakly dependent on the strength of substitution. In the excited triplet states, there are no sites with negative spin densities and the spin densities are more uniform, reflecting higher kinetic energy in the state due to greater spin blocking of the delocalization.

Nonlinear properties

We have computed the linear polarizability $\alpha_{ij}(-\omega, \omega)$ for tetracene and substituted tetracene and the second harmonic generation (SHG) coefficients, $\beta_{ijk}(-2\omega; \omega, \omega)$ for substituted tetracenes, at a frequency corresponding to 0.65 eV. We have employed the correction vector method, which

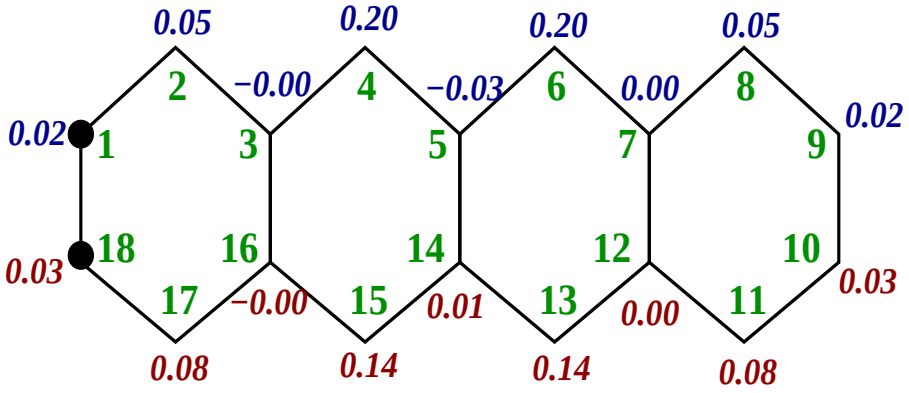

(a)

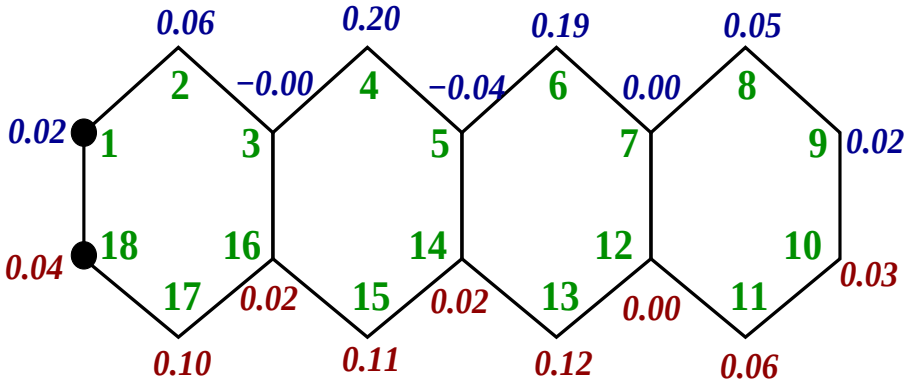

(b)

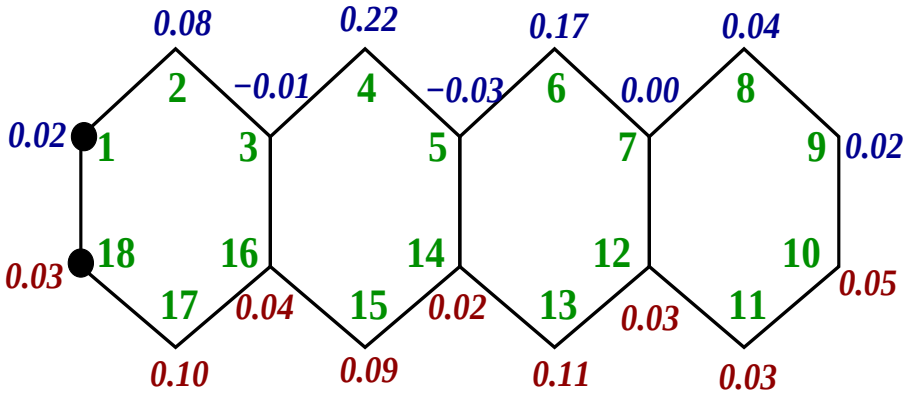

(c)

Figure 6: Spin density for T_1 state (numbers in blue) and optically allowed state (T_2, numbers in red), as a function of site energy, ε. (a) for ε = 0.0 eV, (b) for ε = 2.0 eV and (c) for ε = 4.0 eV. Numbers inside the ring in green represent the site/orbital indices. C_2 symmetry about the long axis is valid for spin densities.

includes all excitations of the model Hamiltonian; the method has been described in detail earlier.[31] We have tabulated only the non-zero and unique components of polarizabilities in 4. We note from 4 that, α_{xx} remains almost independent of substitution strength as the substituents are placed symmetrically about the molecular axis (see 1). The α_{yy} component increases with the substitution strength. The SHG coefficient β_{xxx} is zero, while β_{xxy} and β_{xyx} are equal by permutation symmetry. However, β_{xxy} is not equal to β_{yxx}, because of the substitution along the Y-axis. The β components are in general small, and increases only for strong substitution. The β_{yyy} component is negative for weak substitution but changes sign and becomes comparable to β_{xxy} for strong substitution strength. Although we are not close to resonance at $\omega = 0.65$ eV excitation frequency, the negative sign of β_{yyy} implies that some states with large transition dipoles between excited states have a sign opposite to that of transition dipole with the ground state. These studies indicate that the substituted tetracenes are not good as SHG molecules. The $||\vec{\beta}_{av}||$ value is nearly doubled as the strength of D/A is increased. The excitation energy decreases as we increase the D/A strength while the transition dipole moment increases (see 1), which leads to higher $||\vec{\beta}_{av}||$ with the increase in D/A strength. We have also given a plot of $\vec{\beta}_{av}$ as a function of the laser excitation frequency in 7 for site energy, $\varepsilon = 3.0$ eV. We find that only near the resonance $||\vec{\beta}_{av}||$ has a high value of about 192×10^{-30} esu and the resonance occurs at $E_g/2$, as expected.

Table 4: First order polarizability $\alpha_{ij}(-\omega;\omega)$ and first order hyperpolarizability, $\beta_{ijk}(-2\omega;\omega,\omega)$, as a function of site energy, ε, at $\omega = 0.65$ eV. All quantities are in e.s.u.

ε (in eV)	α_{xx}	α_{yy}	α_{av}	β_{xxy}	β_{yxx}	β_{yyy}	β_{av}
0.0	3.77	1.77	1.85	0.00	0.00	0.00	0.00
1.0	3.63	1.71	1.79	0.86	1.73	-0.43	0.43
2.0	3.66	1.80	1.81	2.16	3.89	-1.30	1.73
3.0	3.67	1.94	1.87	3.89	7.34	-0.86	4.32
4.0	3.66	2.12	1.93	6.04	11.66	1.30	9.50
5.0	3.63	2.28	1.97	8.20	16.84	7.77	18.99
6.0	3.59	2.42	2.00	9.93	21.58	18.99	32.81

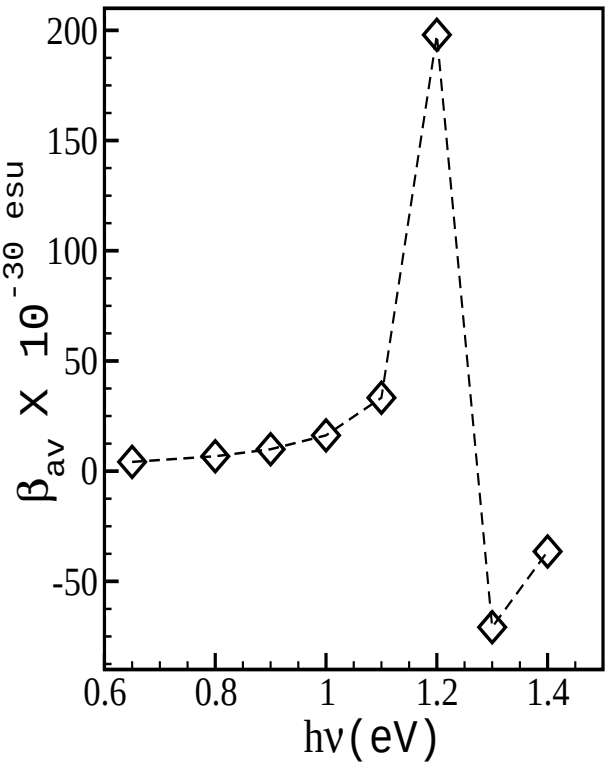

Figure 7: Dependence of the norm of $||\vec{\beta}_{av}||$ on frequency for tetracene for site energy, $\varepsilon = 3.0$ eV.

Summary

Tetracene and substituted tetracenes are important functional molecules. Obtaining reliable low-lying electronic excited states is a major challenge. We have employed the VB method to obtain the singlet and triplet states of the molecules within PPP model. The triplet space dimension is more than 901 million while the dimensionality of the space spanned by the singlets is nearly 450 million. Our studies show that the strongly substituted tetracenes can be useful in organic photovoltaics as they satisfy the energy criteria for singlet fission. The changes in equilibrium geometries of the excited states relative to the ground states are small implying that the Stark shifts will be small. Thus, the excitation energies are close to their value in equi-

librium geometries. The spin density in triplets are mainly confined to the middle of the ring while charge densities of triplets and singlets are large at the substituted sites. The exact SHG coefficients computed for substituted tetracenes show that the SHG response of these molecules are small.

Acknowledgement

We thank Department of Science and Technology, India for financial support (DST0691). Y.A.P. thanks Disha Programme for women in Science, (DST01226) for financial support.

Supporting Information Available

We have given the following figures for site energy $\varepsilon = 3.0$ eV.

i) Charge densities for ground state and dipole allowed vertically excited state.

ii) Difference in charge densities from ground state to vertically excited states in even space and odd space.

iii) Bond order for ground state and dipole allowed vertically excited state.

iv) Difference in bond orders from ground state to vertically excited states in even space and odd space.

v) Charge densities for lowest triplet state and dipole allowed vertically excited state.

vi) Spin densities for lowest triplet state and dipole allowed vertically excited state.

This material is available free of charge via the Internet at `http://pubs.acs.org/`.

References

(1) Lin, Y.-Y.; Gundlach, D. J.; Nelson, S. F.; Jackson, T. N. Stacked Pentacene Layer Organic Thin-Film Transistors with Improved Characteristics, *IEEE Electron Device Letters*, **1997**,

18, 606-608.

(2) Mitsuhashi, R.; Suzuki, Y.; Yamanari, Y.; Mitamura, H.; Kambe, T.; Ikeda, N.; Okamoto, H.; Fujiwara, A.; Yamaji, M.; Kawasaki, N.; Maniwa Y.; Kubozono, Y. Superconductivity in Alkali-Metal-Doped Picene, *Nature*, **2010**, *464*, 76-79.

(3) Okamoto, T.; Suzuki, T.; Tanaka, H.; Hashizume, D.; Matsuo, Y. Tetracene Dicarboxylic Imide and Its Disulfide: Synthesis of Ambipolar Organic Semiconductors for Organic Photovoltaic Cells, *Chem. Asian J.*, **2012**, *7*, 105-111.

(4) Kojima, S.; Okamoto, T.; Miwa, K.; Sato, H.; Takeya, J.; Matsuo, Y. Benzopyrazine-Fused Tetracene Derivatives: Thin-Film Formation at the Crystalline Mesophase for Solution-Processed Hole Transporting Devices, *Organic Electronics*, **2013**, *14*, 437-444.

(5) Bendikov, M.; Wudl, F.; Perepichka, D. F. Tetrathiafulvalenes, Oligoacenes, and Their Buckminsterfullerene Derivatives: The Brick and Mortar of Organic Electronics, *Chem. Rev.*, **2004**, *104*, 4891-4945.

(6) Pope, M,; Swenberg, C. E.; *Electronic Processes in Organic Crystals and Polymers*, Oxford University Press, New York, 1999.

(7) Smith, M. B.; Michl, J. Singlet fission, *Chem. Rev.*, **2010**, *110*, 6891-6936.

(8) Smith, M. B.; Michl, J. Recent Advances in Singlet Fission, *Annu. Rev. Phys. Chem.*, **2013**, *64*, 361-386.

(9) Zimmerman, P. M.; Zhang, Z.; Musgrave, C. B. Singlet fission in pentacene through multi-exciton quantum states, *Nat. Chem.*, **2010**, *2*, 648-652.

(10) Zimmerman, P. M.; Bell, F.; Casanova, D.; Head-Gordon, M. Mechanism for Singlet Fission in Pentacene and Tetracene: From Single Exciton to Two Triplets, *J. Am. Chem. Soc.*, **2011**, *133*, 19944-19952.

(11) Chan, Ti-L; Ligges, M.; Zhu, X-Y. The Energy Barrier in Singlet Fission Can be Overcome Through Coherent Coupling and Entropic Gain, *Nat. Chem.*, **2012**, *4*, 840-845.

(12) Wilson, M. W. B.; Akshay, R.; Bruno, E.; Friend, R. H. Singlet Exciton Fission in Polycrystalline Pentacene: From Photophysics toward Devices, *Acc. Chem. Res.*, **2013**, *46*, 1330-1338.

(13) Burdett, J. J.; Piland, G. B.; Bardeen, C. J. Magnetic field effects and the role of spin states in singlet fission, *Chem. Phys. Lett.*, **2013**, *585*, 1-10.

(14) Wiberg, K. B. Properties of Some Condensed Aromatic Systems, *J. Org. Chem.*, **1997**, *62*, 5720-5727.

(15) Kadantseva, E. S.; Stott, M. J.; Rubio, A. Electronic Structure and Excitations in Oligoacenes; From *ab initio* Calculations, *J. Chem. Phys.*, **2006**, *124*, 134901.

(16) Heinze, H. H.; Görling A.; Rösch, N. An Efficient Method for Calculating Molecular Excitation Energies by Time-Dependent Density-Functional Theory, *J. Chem. Phys.*, **2000**, *113*, 2088-2099.

(17) Raghu, C.; Pati, Y. A.; Ramasesha, S. Structural and Electronic Instabilities in Polyacenes: Density-Matrix Renormalization Group Study of a Long-Range Interacting Model, *Phys. Rev. B*, **2002**, *65*, 155204.

(18) Raghu, C.; Pati, Y. A.; Ramasesha, S. Density-Matrix Renormalization-Group Study of Low-Lying Excitations of Polyacene within a Pariser-Parr-Pople Model, *Phys. Rev. B*, **2002**, *66*, 035116.

(19) Pavlopoulos, T. G. Measurement of the Triplet-Triplet Absorption Spectrum of Tetracene Using cw Argon Laser Excitation, *J. Chem. Phys.*, **1972**, *56*, 227-232.

(20) Kaur, I.; Jia, W.; Kopreski, R. P.; Selvarasah, S.; Dokmeci, M. R.; Pramanik, C.; McGruer, N. E.; Miller, G. P. Substituent Effects in Pentacenes: Gaining Control over HOMO-LUMO Gaps and Photooxidative Resistances, *J. Am. Chem. Soc.*, **2008**, *130*, 16274-16286.

(21) Ishibashi, K.; Iyoda, T.; Hashimoto, K.; Fujishima, A.; Shirai, Y.; Abe, J., First-order Hyperpolarizability of Oligo-Acene Derivatives by Hyper-Rayleigh Scattering, *Chem. Phys. Lett.*, **1997**, *279*, 107-111.

(22) Costa, M. B. S.; Machado, A. E. A; Pavão, A. C. *J. Mater. Sci.*, **2013**, *48*, 192-200.

(23) Ramasesha, S.; Pati, S. K.; Shuai, Z.; Bredas, J. L., The Density Matrix Renormalization Group Method: Application to the Low-Lying Electronic States in Conjugated Polymers, *Adv. Qua. Chem.*, **2000**, *38*, 121-215.

(24) Ramasesha, S.; Soos, Z. G., Diagrammatic Valence Bond Theory for Finite Model Hamiltonians, *Int. J. Quantum Chem.*, **1984**, *25*, 1003-1021.

(25) Soos, Z. G.; Ramasesha, S. Valence-Bond Theory of Linear Hubbard and Pariser-Parr-Pople Models, *Phys. Rev.* , **1984**, *B 29*, 5410-5422.

(26) Ohno, K. Some Remarks on the Pariser-Parr-Pople Method, *Theor. Chim. Acta*, **1964**, *2*, 219-227.

(27) Ramasesha, S.; Soos, Z. G. Magnetic and Optical Properties of Exact PPP States of Naphthalene, *Chem. Phys.*, **1984**, *91*, 35-42.

(28) Biermann, D.; Schmidt, W. Diels-Alder Reactivity of Polycyclic Aromatic Hydrocarbons; Acenes and Benzologs, *J. Am. Chem. Soc.*, **1980**, *102*, 3163-3173.

(29) Katul, J.; Zahlan, A. B. Tetracene Dimer, *J. Chem. Phys.*, **1967**, *47*, 1012-1014.

(30) Tomkiewicz, Y.; Groff, R. P.; Avakian, P. Spectroscopic Approach to Energetics of Exciton Fission and Fusion in Tetracene Crystals, *J. Chem. Phys.*, **1971**, *54*, 4504-4507.

(31) Soos, Z. G.; Ramasesha, S. Valence Bond Approach to Exact Nonlinear Optical Properties of Conjugated Systems, *J. Chem. Phys.*, **1989**, *90*, 1067-1076.